Chapter 14

HIGH-TEMPERATURE STABLE NANOPARTICLES DEMONSTRATED ON SELF-CLEANING TITANIA COATINGS

Alfred P. Weber[1], Fei Qi[1], Anna Moiseev[2]
and Joachim Deubener[2]
[1]Institute of Particle Technology, TU Clausthal, Germany
[2]Institute of Non-Metallic Materials, TU Clausthal, Germany

ABSTRACT

While the unique properties of nanoparticles are employed in an uncountable number of applications their use at high temperatures is limited by their thermal stability. Encapsulation of the nanoparticles with a protective layer can reduce particle sintering but, at the same time, renders the surface inaccessible for reactive species as for instance desired in heterogeneous catalysis. Therefore, this chapter aims at the introduction of a one-step flame process to produce high temperature stable titania nanoparticles with a silica coating. It was found that grain growth and phase transformation from active anatase into inactive rutile phase was inhibitedup to 1050°C. The heat treatment was necessary to obtain a permeable coating, as proven by the decomposition of organic compounds. In fact, for each application temperature an optimum layer thickness exists for maximum photocatalytic activity. It was shown that high temperature stable and self-cleaning-coatings can be achieved by spray coating of silica wafers. The concept of high temperature stabilization by hermetic coating could be refined for pure interparticle contact passivation and extended to other material systems such as metal nanoparticle catalysts.

1. INTRODUCTION

Due to their high surface energy small solid nanoparticles are inherently unstable upon heating as reflected in reduced melting point [1, 2], enhanced coalescence [3] and facilitated phase transition[4, 5].The thermal instability of nanoparticle restricts their high temperature

processing, e.g. the co-firing of functional coatings such as self-cleaning surfaces, and limits their application temperature in catalysis [6, 7]. The reduction of the particle surface energy can be achieved by surface decrease due to sintering or by coating the particle with a material exhibiting a lower surface energy. For metal nanoparticles, besides coating, particle alloying and immobilisation on an oxide support are used to stabilize the nanoparticles at higher temperatures. At low temperatures (<300°C), organic capping agents can be used as protection against sintering and deactivation of the catalysts nanoparticles. As a consequence of the particle surface shielding reduced activities due to diffusion limitations and blocking of active sites have to be faced[8]. Moreover, for many applications, the optimum reaction temperatures are much higher so that the capping agents start to decompose followed by the loss of active catalyst surface due to crystallite growth. To achieve stability at higher temperatures metal oxide coatings were applied with sol-gel techniques [9] leading to Pd nanoparticles encapsulated in silica. Suryanarayanan et al. studied the microporosity of silica coatings on noble metal nanoparticles produced by sol-gel method [10]. Despite of the absence of a direct evidence by high resolution TEM imaging they concluded that pore sizes below 1 nm of the shell material allow small molecules to permeate while blocking larger ones. However, all of the presented sol-gel techniques require a tedious chain of single steps leading to expensive and time-consuming processes [9]. Therefore, simple generic approaches to synthesize technical relevant quantities of nanoparticles with increased thermal stability at high temperatures are highly desired with the constraint to keep the particle surface accessible for reactive species. As an alternative to the sol-gel processes flame synthesis is a versatile technique for the production of nanopowders, which is employed in industry with worldwide yields of megatons per year [11]. Based on the pioneering work of Pratsinis [11-19] over the last decade the range of flame synthesized nanoparticles has been extended towards complex structures such as core-shell particles, nanotubes and nanowires of various compositions.

In this chapter the influence of nanoparticle coatings on the opposing effects of improved thermal stability and reduced surface accessibility is discussed on the example of flame synthesized titania nanoparticles coated with silica for photocatalytic applications. As indicator for the surface access the photocatalytic activity is taken. The high temperature stability of the TiO_2/SiO_2 nanoparticles is required to realize for instance the industrial procedure for the manufacturing of roof tiles with self-cleaning coatings in one step where the nanoparticles have to withstand temperatures over 950°C for many hours without substantial loss in photocatalytic activity. The obtained self-cleaning effect of roof tiles is based on the combination of photocatalytic oxidation of organic compounds and super-hydrophilic character of the surface. The behaviour of non-stabilized titania nanoparticles is shown for the commercial nanopowder P25 (Evonik, Germany) in Figure 1. While this powder exhibits particles sizes of about 20 nm and 80 wt.% anatase content before heat treatment (a), the particles increase significantly in size and transform completely to inactive rutile phase when exposed up to 1000°C for 3 h (b). The goal of this contribution is to outline a way to avoid such phase transformation and particle growth through particle coating.

Firstly, the flame synthesis of the titania/silica core/shell nanoparticles will be presented including the experimental setup and the characterization methods. Then, after optimizing the photocatalytic activity of the pure titania particles, the high temperature stability of the TiO_2/SiO_2 nanoparticles will be discussed. Afterwards, the photocatalytic activity of the

calcinated TiO_2/SiO_2 nanoparticles and the self-cleaning properties of TiO_2/SiO_2 coatings will be presented.
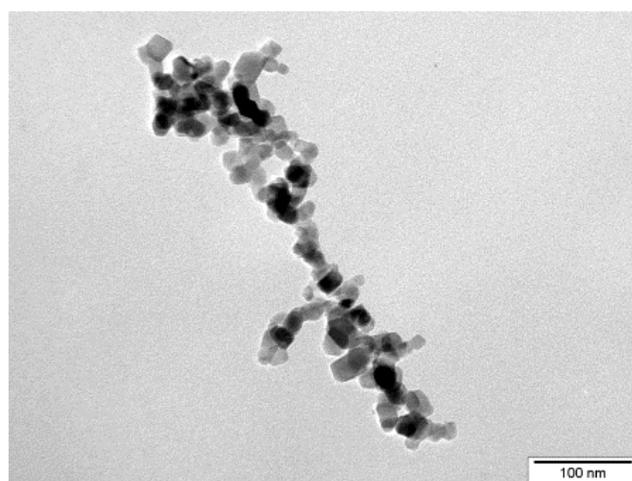
(a) TiO_2 P25, before calcination
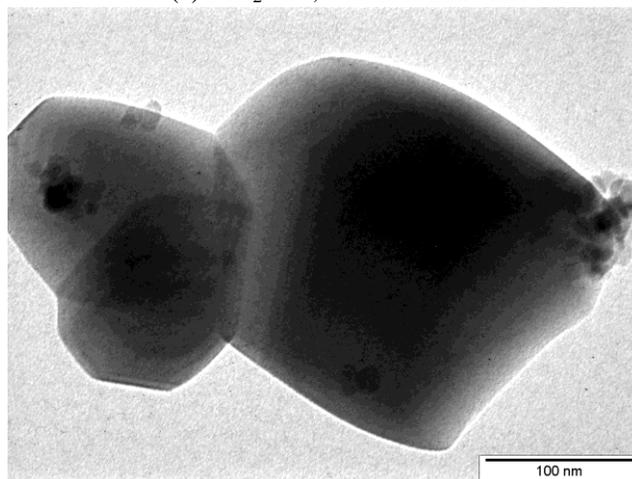
(b) TiO_2 P25, 900 °C, 3hours

Figure 1. TEM micrographs of commercial titania nanoparticles P25 (Evonik, Germany) before (a) and after (b) heat treatment (scale bars correspond to 100 nm).

2. FLAME SYNTHESIS OF STABILIZED TITANIA NANOPARTICLES

Titania nanoparticles are for instance employed in photovoltaics [20], self-cleaning surfaces [21, 22], antibacterial coatings [23, 24] and water/air purification [25]. Due to their strong UV absorption titania nanoparticles are also used for UV protection in sunscreen, cosmetic products, textile fibers and coatings of plastics. However, here the catalytic activity induced by the absorption of UV photons is not desired and catalytic effects on skin or on polymer panels are avoided by hermetically surrounding the titania nanoparticles with an impermeable coating such as SiO_2 [26]. For this purpose, Teleki and Pratsinis [27] developed

a flame synthesis process for TiO_2/SiO_2 nanoparticles. To obtain a homogeneous coating the mixing of the coating precursor gases ($SiCl_4$) in the flame was investigated in details by computational fluid dynamics (CFD) simulations and the precursor feeding geometry was optimized experimentally [28]. However, since the application of these composite nanoparticles was intended for room temperature, the behavior of the core-shell-nanoparticles at high temperatures, where crystal growth and phase transformation of titania may be encountered, was not investigated further. Principally, TiO_2 is polymorph with the two main modifications of anatase and rutile. Upon heating photocatalytically active anatase transits irreversibly to hardly active rutile at temperatures over 400°C. The transformation kinetics is influenced by grain size, impurities and reaction atmosphere [29]. The basic idea of the approach here is to inhibit coalescence and phase transition by passivating the contact zone between titania nanoparticles with a silica layer [30, 31]. While similar approaches have been undertaken in complex and lengthy liquid phase syntheses of titania/silica core/shell nanoparticles, a simple gas phase synthesis for fast and continuous one step production with facile scale-up will be presented here.
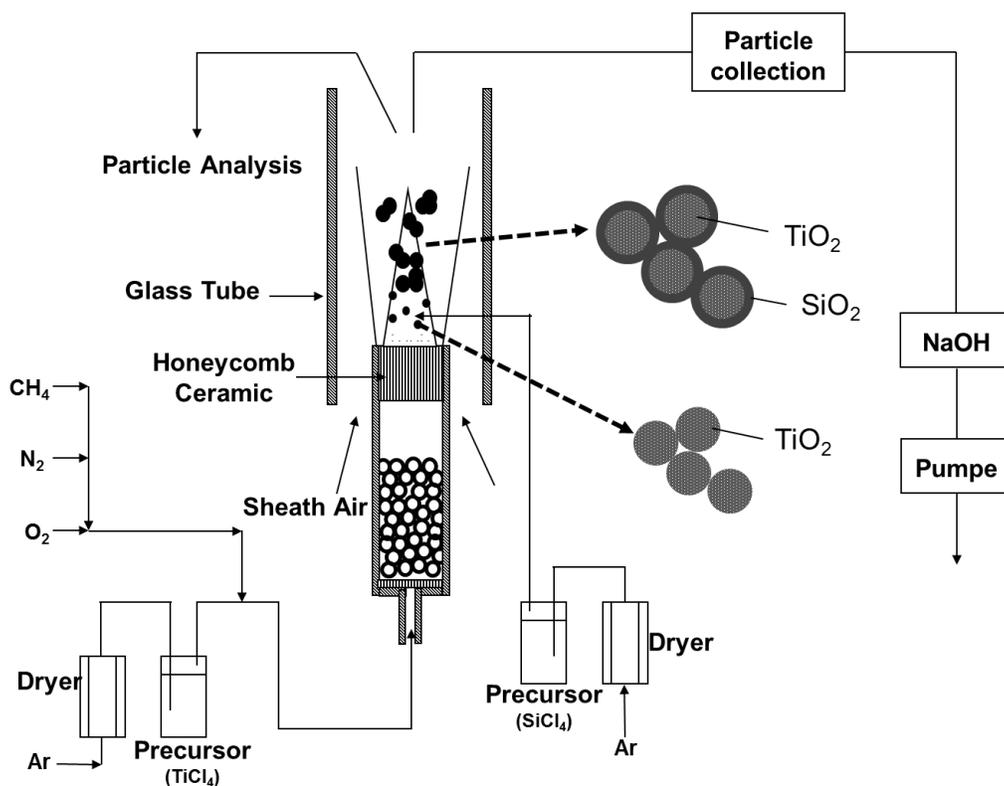

Figure 2. Schematic setup for flame synthesis of core-shell TiO_2/SiO_2 nanoparticles.

Figure 2 shows the experimental setup. The main part is the laminar flat flame burner where the titania precursor($TiCl_4$) is oxidized in a methane/oxygen/nitrogen premixed flame. To obtain the SiO_2 coating on the TiO_2 nanoparticles a second precursor ($SiCl_4$) is added at a higher position in the flame where the formation of the titania particles is completed. After

fast decomposition of the $SiCl_4$ the formed SiO_2 condenses on the surface of the TiO_2 nanoparticles to form a core-shell structure (Figure 3).

The burner is made of a quartz glass tube filled with quartz glass spheres for homogeneous gas mixing and a honeycomb ceramic guaranteeing a laminar flame. Besides methane as fuel gas and oxygen as oxidant nitrogen was introduced as balance gas raising the flame above the burner. The precursor gases ($TiCl_4$ and $SiCl_4$) were controlled by saturating dry argon flows through bubblers containing the liquid precursor at room temperature. All flow rates were controlled with mass flow controllers. The visible flame height was about 10 mm and the maximum temperature was about 1000°C as measured in absence of the titanium tetrachloride vapour. The generated particles were collected on a glass fibre filter placed in a stainless steel filter holder connected to a vacuum pump and fixed about 50 cm above the flame. For neutralization the exhaust stream passed through a sodium hydroxide solution.
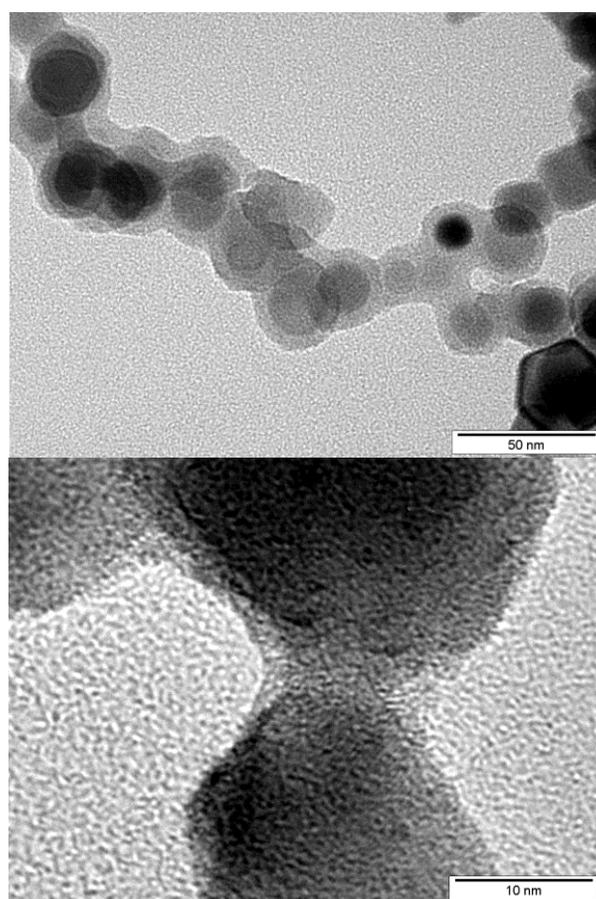

Figure 3. (above) Core-shell structure of TiO_2/SiO_2 nanoparticles and (below) silica deposited in the contact zone between two titania nanoparticles.

As a widely employed reference material for titania nanoparticles P25 (Evonik, Germany) was used. The morphology of reference material and flame synthesized TiO_2/SiO_2 particles was examined by transmission electron microscopy (TEM, JEM 2100, JEOL) operated at 120 KV und scanning electron microscopy (SEM, Zeiss, DSM 982 Gemini). The

specific surface area (SSA) of synthesized powders was determined from a five-point nitrogen adsorption isotherm obtained from Brunauer-Emmett-Teller (BET) measurements using a Gemini 2360 (Micromeritics, USA). Prior to analysis powders were degassed at 120°C for two hours.X-ray diffraction (XRD) was used for crystal phase identification. The relative weight fraction of anatase phase (W_A) was calculated using Spurr and Meyers formula with the relative intensity of the anatase peak(I_A) ($2\theta = 25.3°$) and rutile peak (I_R) ($2\theta = 27.4°$). The evaluation of photocatalytic activity was carried out in aqueous phase by monitoring the decomposition of dichloroacetic acid (DCA) and 4-chlorophenol (4-CP)used as model substances due to the photocatalytic oxidation. For this purpose total organic carbon (TOC) of the solution was measured with Analytic-Jena IDC-micro N/C TOC-Analyzer. The measurements of zeta potential of TiO_2 catalyst dispersed in distilled water as a function of pH value were carried out with Malvern Zetasizer (Nano series) torecord the change of SiO_2 layer along with heat treatment.
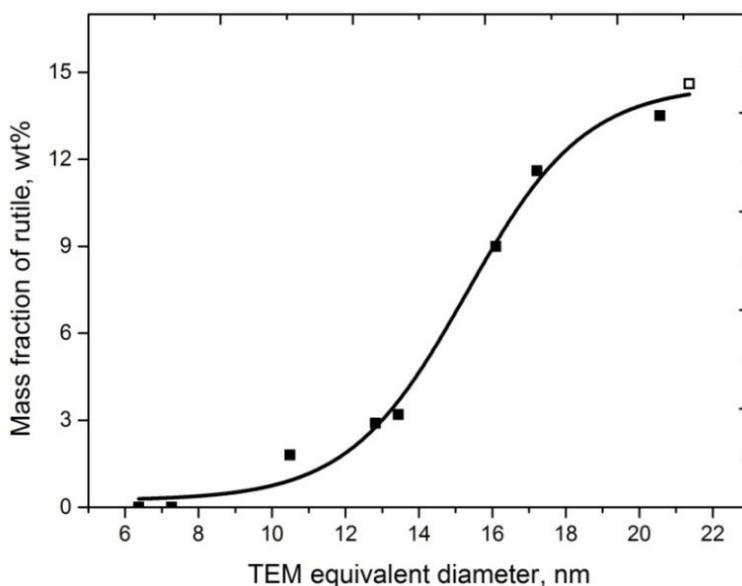

Figure 4. Mass fraction of rutile as function of the particle size for home-made titania (filled squares) and for commercial titaniaP25 (open square).

3. OPTIMIZATION OF THE PHOTOCATALYTIC ACTIVITY OF PURE TITANIA PARTICLES

Generally, the photocatalytic performance of TiO_2 is affected by particle properties such as particle size, surface area, phase composition and conditions of photocatalytic tests such as concentration of photocatalyst [32-36]. The conditions of photocatalytic tests can be well controlled, whereas the particle properties depend on the configuration and properties of flame, for example, precursor type and concentration, flame height and temperature, particle residence time in the flame. For a co-flow diffusion flame (CH_4/air) Pratsiniset al.have found that the flame configuration, fuel and oxidant flow rates as well as precursor concentration of

TiCl$_4$ have a profound effect on the particles properties [13]. They observed that the gas mixing influenced flame height andflame temperature affecting particle surface area and size. For the same flame configuration, Akurati et al. have investigated the influence of titanium tetraisopropoxide (TTIP) precursor concentration and oxygen flow rate on particle properties [37]. It was found that the specific surface area of the synthesized TiO$_2$ increased with increasing oxygen flow rate indicating lower flame temperature, as theflow rates of lift gas N$_2$ and fuel gas CH$_4$ were kept constant. In addition, the specific surface area of TiO$_2$ decreased with increasing precursor concentration as a consequence of higher flame temperatures induced by the exothermic oxidation of TTIP. For the less variable configuration of a premixed flame, the particle properties are mainly influenced by precursor type and concentration, flame temperature and residence time of the particles in the flame [38]. The particle properties may also be affected by electrical fields applied to the flame. For a CH$_4$/O$_2$ premixed flame Katzer et al. have shown that an increase of the electric field strength resulted in a decreased primary particle size and in a reduced rutile mass fraction of titania particles [39]. In addition to TiO$_2$ particles, electrical fields were also employed to affect the properties of silica, carbon and silica-carbon composites synthesized in flame reactors [40, 41].

In the study presented here, the size of the titania particles was adjusted between 7 and 22nm by varying the TiCl$_4$ precursor flow rate. However, with changing synthesis conditions also the rutile content changed. The correlation between rutile mass fraction and TEM equivalent primary particle diameter is shown in Figure 4. With increasing particle size the rutile content increases but levels off for diameters above 20 nm. Since the anatase-to-rutile transition depends on the synthesis temperature, the maximum rutile fraction obtained in the employed configuration is limited to 14wt.% due to the low temperature and short residence time in the flame. However, the critical diameter where substantial transformation sets in was found to be around 14 nm, which is in good agreement with literature [4, 42]. Also the commercial titania reference material P25 fits with the curve of the home-made titania.

The photocatalytic activity was measured by fitting the kinetics of the decomposition of the organic compound i with a first order reaction.

$$TOC(t) = TOC_0 \cdot \exp(-k_i \cdot t)$$

where TOC$_0$ is the initial concentration of the compound i (i=DCA or 4-CP), k$_i$ is the reaction rate constant for compound i and t is the duration of the reaction. The measured dependence of the photocatalytic activity on the particle size is shown in Figure 5.

For both reactions an optimum particle diameter of the titania of about 14 nm is observed for a given catalyst mass. Although the anatase content changes with particle size (from 100 to 86 wt.% as shown in Figure 4) it was found that the dominant parameter for a high photocatalytic activity is the particle size. Therefore, the synthesis conditions for the titania core particles with high activity were retained for the subsequent coating experiments with silica.
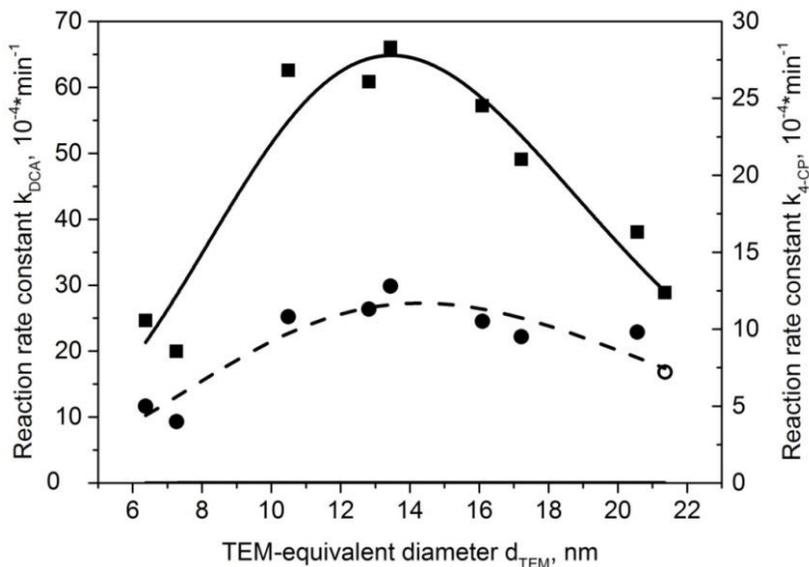
Figure 5. Reaction rate constants for the decomposition of DCA (left axis) and 4-CP (right axis) as function of the titania particle diameter for home-made titania (filled symbols) and for commercial P25 (open symbols).

4. HIGH TEMPERATURE STABILITY OF TITANIA NANOPARTICLES

It is well known that anatase is the most photocatalytically active modification of TiO_2 particles [43, 44]. However, the non-stabilized TiO_2 nanoparticles are only suitable for efficient photocatalytic application up to 600°C excluding processing or applications at higher temperatures. As shown in Figure 1, high temperatures result in a sintering induced loss of small anatase particles, which is the favored form in flame synthesis [45, 46]. The sintering rate of TiO_2 particles depends on particle size and temperature. Nakaso showed that the onset temperature for small particles is lower than for larger ones, when the residence time is long enough for the sintering process [47]. Zhang and Banfield have reported that the phase transformation for nanoparticles occurred at 250°C while for millimeter particles the temperature is much higher (900°C) [48]. The corresponding activation energy is above 400 kJ/mol for macroscopic particles [49] butonly147 kJ/mol for ultrafine anatase particles [48]. Once the phase transformation due to particle sintering has started, the rutile fraction increases exponentially because of the further local temperature increase due to the energy release as consequence of the surface reduction [50]. These results are consistent with the studies of Zhang and Banfield [42, 51].

To improve the thermal stability of TiO_2 particles different approaches were developed. On one hand, to avoid impurities in the particles the synthesis processes was modified without additives [17, 44, 52-54]. The authors showed that the TiO_2 synthesized in the liquid phase was stable up to about 800°C. However, these TiO_2 particles are still not suitable for the applications in ceramic processes above 950°C. On the other hand, additives such as SiO_2were used to extend the thermostability of TiO_2 [6, 55, 56]. They showed the high

thermostability of TiO_2 particles connected with SiO_2 via Ti-O-Si bonds up to 1200°C, but with stability lasting only for 30 min. According to the studies of Shannon et al. and Okada et al., the anatase particles should be separated by a passivation layer to achieve high stability by suppressing diffusion between anatase particles in direct contact [30, 57]. In the present contribution, TiO_2 particles were stabilized by interface passivation as SiO_2 formed amorphous protection layers on the TiO_2 particles.

Figure 6 shows the anatase mass fraction of TiO_2 particles coated with silica layers of different thickness as a function of calcination temperature. The anatase mass fraction is taken as indicator for the thermostability of stabilized TiO_2 nanoparticles. It is observed that all TiO_2/SiO_2 samples are stable up to 950°C exhibiting the same anatase mass fraction after calcination, independently of the silica layer thickness. For calcination temperature above 950°C the anatase mass fraction decreases rapidly. Nevertheless, the onset of the anatase-to-rutile transformation is shifted to higher temperatures with increasing SiO_2 layer thickness. For the sample with thick silica layers (8.7 nm), the particles are stable up to a temperature of 1050°C, while for the sample with thin silica layers (1.6 nm) the thermostability is limited to 950°C.
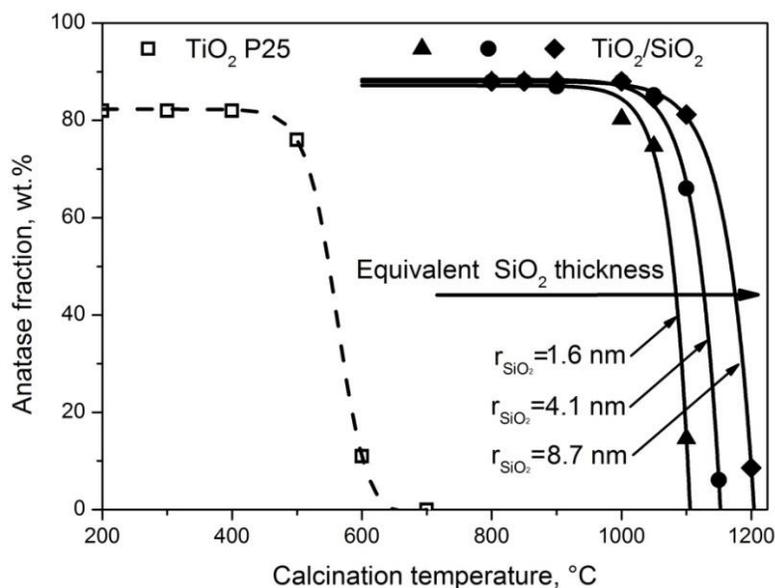

Figure 6. Influence of calcination temperature on the phase composition of non-stabilized TiO_2(P25) and stabilized TiO_2 nanoparticles with different thickness of SiO_2 layer.

The thermostability is not only reflected in the conservation of the anatase phase but also evidenced by the behavior of the TiO_2 particle size as a function of calcination temperature (Figure 7). For the core-shell TiO_2/SiO_2 particles the size of the TiO_2 cores, which was optimized to maximum photocatalytic activity, stays approximately constant up to the calcination temperature of 1050°C. When the calcination temperature exceeds the critical point of 1050°C, the SiO_2 layer is assumed to decay into small droplets releasing a substantial

part of the titania surface which allows the titania particles to sinter quite rapidly. Such a disintegration of metal oxide coatings was already observed for SnO_2 films, however, at much lower temperatures [58]. In comparison to the stabilized TiO_2 samples, the non-stabilized TiO_2 particles show the same trend of particle growth, which is also reported by [52] and [59]. The difference is that the onset temperature of particle growth for non-stabilized TiO_2 particles is reduced by about 500°C compared to the stabilized titania nanoparticles.
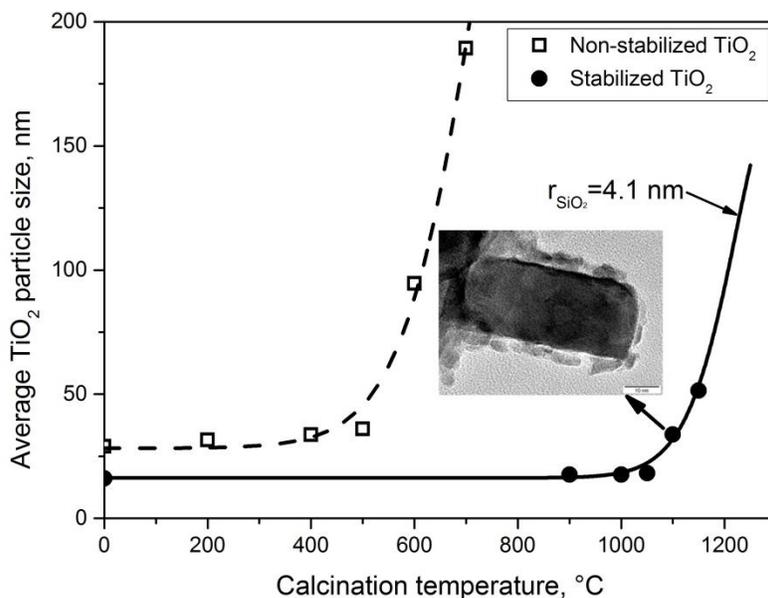

Figure 7. Influence of calcination temperature on the particle size of non-stabilized TiO_2 P25(open symbols) and stabilized TiO_2 nanoparticles(filled symbols).

On the one hand, the results of Figure 7 show the disintegration of the protective silica coating at higher calcination temperatures. On the other hand, our results on photocatalytic activity (see next chapter) indicates that without calcination the silica coating is not permeable for reactive species, i.e. there is an hermetic enclosure of the titania core. Therefore, the question arises how the silica layer behaves in the temperature range between 900°C and 1050°C, where high photocatalytic activity is observed (Figure 10).

An approach to determine the quality of the silica coating, i.e. the barrier for accessing the titania surface, was proposed by Furlong et al. and further developed by Teleki et al. [27, 60]. They characterized the quality of SiO_2 layer by measuring the zeta potential as a function of the pH value. Furlong et al. showed that the isoelectric point (IEP, where the zeta potential becomes zero) of coated TiO_2 particles was shifted to the IEP of pure SiO_2 with increasing SiO_2 content (from 0.2 to 5 wt.%). For silica contents above 2.5 wt.%, the IEP of TiO_2/SiO_2particles reached the IEP of pure SiO_2 (at pH=3.1) indicating an hermetic encapsulation of the titania particles with silica layer.

We employed this technique to investigate the behavior of our TiO_2/SiO_2nanoparticles. As shown in Figure 8, the IEP of stabilized TiO_2 particles was similar to the IEP of pure

SiO_2, which means that the TiO_2 particles were hermetically coated with an impermeable SiO_2 layer. After calcination at 1000°C the IEP of TiO_2/SiO_2 particles was shifted towards to the IEP of pure TiO_2, indicating that the TiO_2 surface was released by heat treatment. However, based on these results it cannot definitively be decided whether the silica layer becomes porous (maybe with some cracks) or the silica retreats due to lowered viscosity at high temperature treatment.
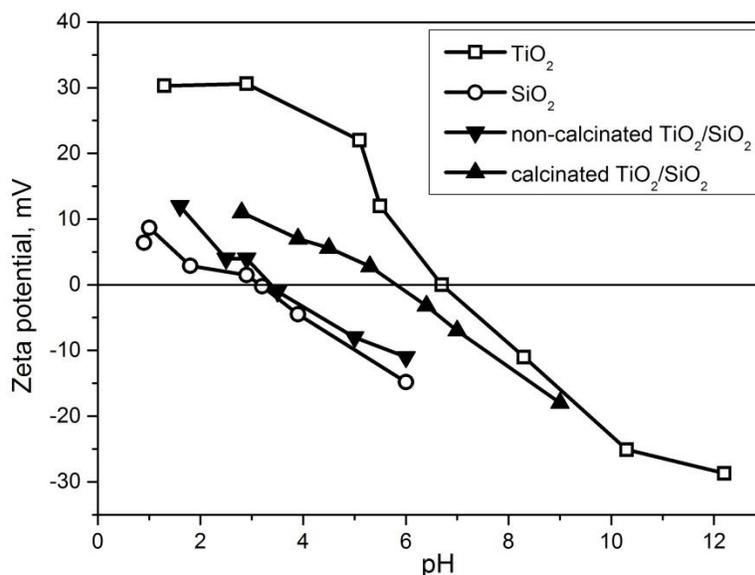

Figure 8. Influence of calcination on zeta potential as a function of pH value of TiO_2/SiO_2 particles.

However, the results show that the interface passivation with SiO_2 can be widely used to prevent sintering of metal or metal oxide catalyst for applications at high temperatures [61], for example, to enhance the thermostability of Pt particles in gas sensors [62] when the surface access can be established.

5. PHOTOCATALYTIC PROPERTIES OF TITANIA NANOPARTICLES

For many applications the relevant feature of TiO_2 nanoparticles is their photocatalytic activity. The photocatalytic degradation of organic compounds occurs at the TiO_2 surface by either indirect oxidation via the surface-bound hydroxyl radical or directly via the valence-band hole [63-65]. The commercial product of TiO_2 P25 from Evonik exhibits high activity because of its high surface area (50 m^2/g) and high anatase content (80 wt.%) and, therefore, it is widely used as reference material for comparison of photocatalytic activity.

In the presented experiments the photocatalytic activity was evaluated by degrading of DCA in water as model organic substance under the irradiation of a UV-A light. Figure 9 shows an example of photocatalytic degradation of DCA with calcined non-stabilized and stabilized

TiO_2photocatalysts. The non-stabilized TiO_2P25 showed negligible photocatalytic activity after calcination at 900°C for 3 hours indicating that the application of TiO_2 P25 is limited to temperatures below 900°C. The result agrees with the observation of phase composition and particle size of TiO_2 P25 calcinated at various temperatures (Figures 6 and 7).
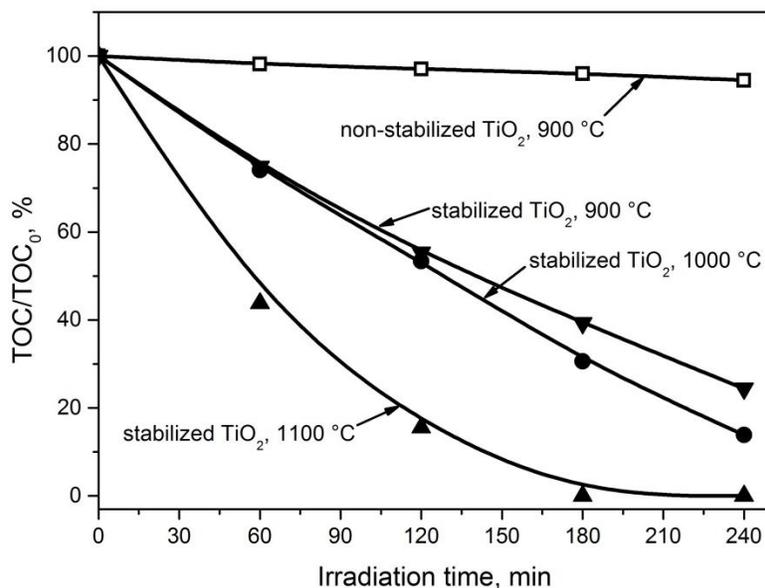

Figure 9. Photocatalytic degradation of DCA with calcinated non-stabilized TiO_2 P25 and stabilized TiO_2 nanoparticles.

According to the study of El-Toni et al. [26], TiO_2 particles passivated with hermetic SiO_2layer on the surface show no photocatalytic activity because the TiO_2 particles have no contact with organic compounds. Based on this barrier effect coated TiO_2 particles are used for example in pigments or in sunscreens. However, in photocatalysis the TiO_2 surface needs to be accessible for the reacting molecules. This access was, at least partially, achieved by heat treatment as indicated by the shift of the IEP of calcinated TiO_2/SiO_2particles towards the value of free TiO_2 surfaces (Figure 8). The same conclusion results from activity measurements shown in Figure 9, where the core-shell TiO_2/SiO_2 particles show high photocatalytic activity after calcination. The TiO2/SiO_2 particles calcinated at 1000°C show higher photocatalytic activity than the particles calcinated at 900°C indicating that more surface was released at higher temperature. However, after heat treatment at 1100°C the SiO_2 layer was destroyed (cf. Figure 7) causing phase transformation and sintering leading to reduced photocatalytic activity.
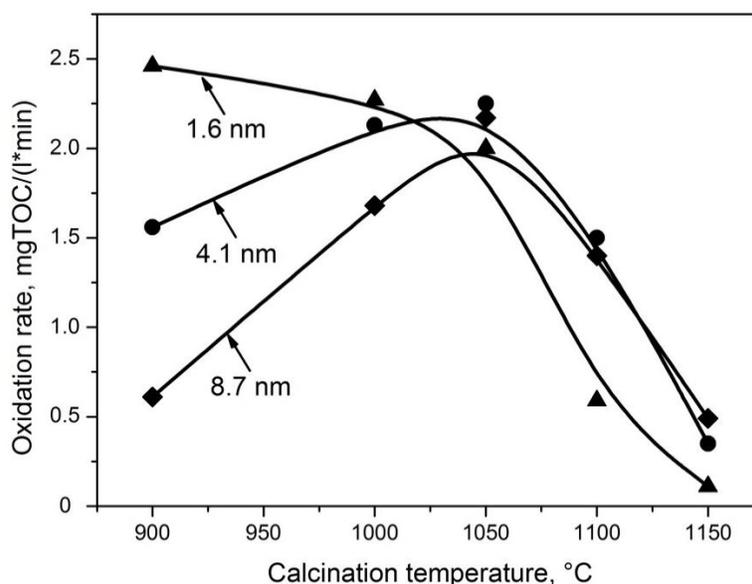
Figure 10. Influence of calcination temperature on the photocatalytic activity of TiO_2/SiO_2 particles with SiO_2 layers of different thickness.

Figure 10 shows the effect of the calcination temperature on the DCA oxidation with TiO_2 particles stabilized with different silica content. For the TiO_2 particles coated with a thin silica layer (1.6 nm) the DCA oxidation rate decreased steadily with the increasing calcination temperature, due to an insufficient protection of SiO_2 layer against sintering and phase transformation. For the samples with thicker silica coatings (4.1 nm and 8.7 nm), the DCA oxidation rate first increases with calcination temperature, reaches a maximum at about 1050°C and decreases with further increased calcination temperature. The maximum value of DCA oxidation rate is first shifted to higher temperatures with increasing silica content. However, for temperatures above 1050°C the activity steadily drops with temperature independent of the silica layer thickness. While at lower temperatures the increase of DCA oxidation with temperature is due to increasing release of accessible TiO_2 surface, the activity drop at higher temperatures is a consequence of the disintegration of SiO_2 either by cracking or retracting movement resulting in phase transformation and particle growth. In the temperature range below such disintegration phenomena of the silica coating, the DCA oxidation rate decreases with increasing SiO_2 layer thickness due to an enhanced barrier effect.

6. APPLICATION OF TITANIA NANOPARTICLES FOR SELF-CLEANING COATINGS

In recent years, coatings of TiO_2 nanoparticles have attracted attention as self-cleaning surfaces where adsorbed organic pollutants are decomposed under UV irradiation and the contaminant as well as dust is washed off by rainwater. Based on the combination of

photocatalytic oxidation and excellent wetting (i.e. superhydrophilic behavior)surfaces of buildings may stay clean for extended periods of time. However, while the TiO_2 coating can be applied at room temperature, a long-lasting coating adhesion to the support is obtained only after simultaneous calcinations of coating and substrate, where the coating quality (i. e. the lifetime) increases with temperature.
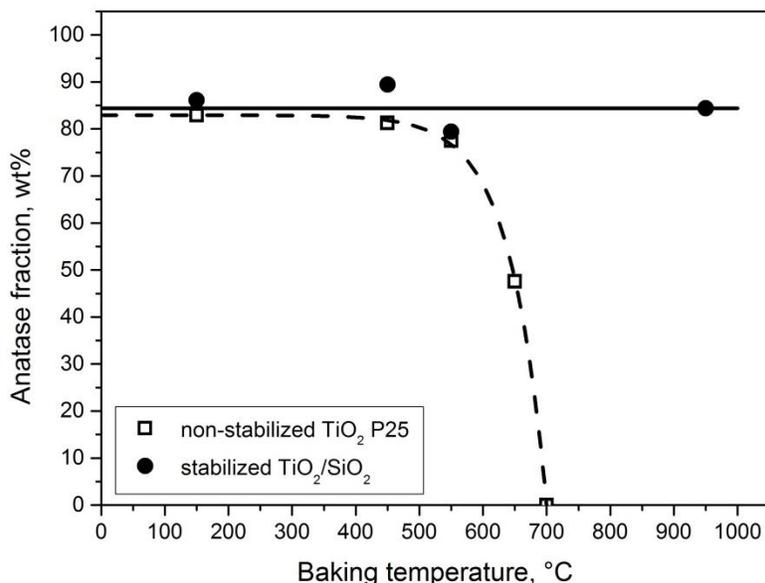

Figure 11. Influence of baking temperature of coatings on the phase composition of stabilized TiO_2 nanoparticles compared to TiO_2 P25.

For industrial realization the coating is intended to be applied in one step to save energy, time and costs. The stabilized TiO_2 nanoparticles were applied for self-cleaning surfaces on silica wafer as model substrate by spray coating. As shown in Figure 11, the phase composition of the coatings with temperature was the same as determined for the original powders (cf. Figure 3) suggesting that neither the coating process nor the substrate has an influence on the thermostability of the tested powders, which is also reported by Hofer et al. [55]. After baking above 700°C, the TiO_2 P25 coating has completely lost the anatase phase, whereas the TiO_2/SiO_2 coating shows a constant anatase mass fraction at least up to 950°C.

Figure 12 shows the photocatalytic activity of coatings from non-stabilized TiO_2 P25 and stabilized TiO_2/SiO_2as a function of baking temperature. The P25 coating exhibits high photocatalytic activity up to 600°C. At higher temperatures the P25 activity drops rapidly to zero. In contrast to this behaviour, the activity of the coating from stabilized TiO_2/SiO_2increases with baking temperature, reaches the maximum at 750°C and decreases slowly for higher temperatures. Although, the maximum activity of the stabilized TiO_2/SiO_2 coating is lower than the maximum of P25 coating, its working range extends significantly further into the high temperature range, in which the P25 coating is totally inactive.
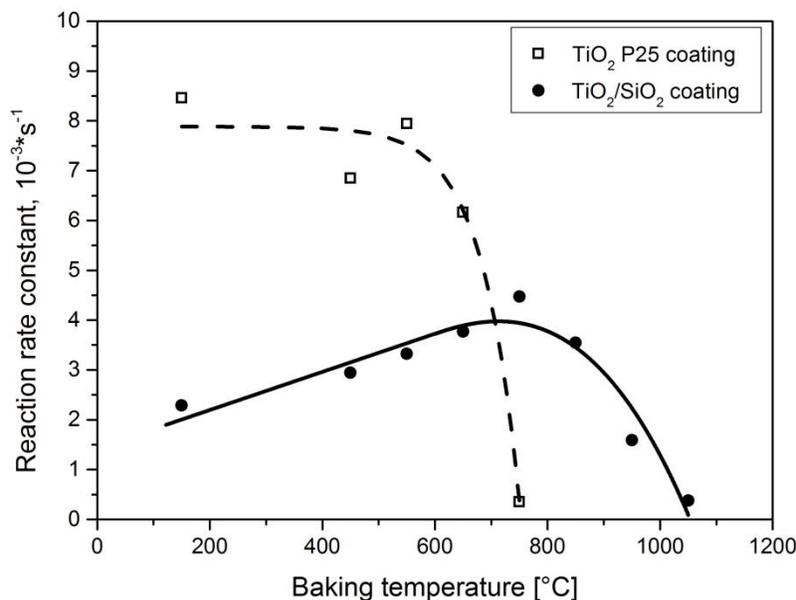
Figure 12. Rate constant of DCA degradation with TiO$_2$ P25 and TiO$_2$/SiO$_2$ coatings as a function of the baking temperature.

The evaluation of the XRD spectra showed that there is neither a change in the phase composition (Figure 11) nor in the primary particle size (not shown here). Also the principle dependency of the photocatalytic activity on calcination temperature is the same for the TiO$_2$/SiO$_2$ coatings (Figure 12) and for the original powders (Figure 10). However, the drop of the photocatalytic activity starts at low temperatures for the self-cleaning coating (at about 750°C) compared to the original powders with the same silica layers thickness (at about 900°C). The reason for this behaviour is so far unclear but may be related to the porous structure of the self-cleaning coating. As indicated in Figure 13, which represents a cross section through the coating, silica draining from the upper TiO$_2$/SiO$_2$ particles for temperature above 750°C may reduce the surface accessible for catalytic reaction.

The self-cleaning effect is based on the combination of photocatalytic activity and good wetting. While the remaining activity of TiO$_2$/SiO$_2$ coatings after calcination was presented above, the wettability of the coatings was tested using the sessile drop method. This technique allows to determining the contact angle which is an indicator of the wetting behavior. It was found that even without UV irradiation the contact angle of the TiO$_2$/SiO$_2$ coatings was below 10° which indicates very good wetting. Additional irradiation with UV light, which originates from the sun light and which is needed for the photocatalytic effect, increases the wettability by further reducing the contact angle. Therefore, it can be concluded that the synthesized TiO$_2$/SiO$_2$ coatings not only exhibit high thermal stability but also self-cleaning properties when applied to extended surfaces and exposed to high temperatures.
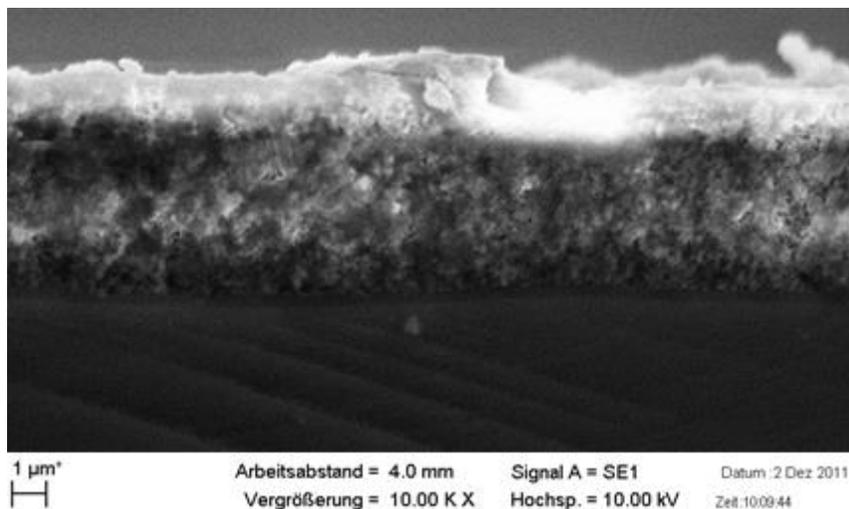
(Scale bar corresponds to 1 μm).

Figure 13. SEM micrograph of the porous structure of TiO_2/SiO_2 coating before baking.

CONCLUSION AND OUTLOOK

In this contribution it was shown that photocatalytically active titania nanoparticles can be conditioned by interface passivation for high temperature applications and processes.

As a simple technique with the potential for scale up to high yields flame synthesis was used to produce silica coated titania nanoparticles with high thermostability. It was shown that up to 1050°C grain growth and phase transformation from active anatase to inactive rutile was inhibited. However, the silica coating layer becomes permeable for reactive species only after heat treatment, as shown by the decomposition of organic compounds. While an increase of silica layer thickness improved the thermostability of TiO_2 particles, the permeability of silica layer decreased at the same time. Therefore, an optimum layer thickness exists for each application temperature as compromise between thermostability and photocatalytic activity.

For application as self-cleaning coatings the stabilized TiO_2 particles showed also high thermostability up to 1050°C and higherphotocatalytic activity compared to reference material TiO_2 P25. In addition, a good wettability of the TiO_2/SiO_2 particle coatings was observed.

Based on the described results, this concept of high temperature stabilization can be refined for pure contact passivation and extended to other material systems such as metal nanoparticle catalysts.

ACKNOWLEDGMENT

REFERENCES

[1]   Pawlow, P., Über die Abhängigkeit des Schmelzpunktes von der Oberflächenenergie eines festen Körpers. *Z. Phys. Chem.,* 1909. 65: p. 1-35.

[2]   Pawlow, P., Über die Abhängigkeit des Schmelzpunktes von der Oberflächenenergie eines festen Körpers (Zusatz). *Z. Phys. Chem.,* 1909. 65: p. 545-548.

[3]   Buffat, Ph. and Borel, J.-P., Size effect on the melting temperature of gold particles. *Phys. Rev.* A, 1976. 13: p. 2287-2298.

[4]   Zhang, H. and Banfield, J. F., Thermodynamic analysis of phase stability of nanocrystallinetitania. *J. Mater. Chem.,* 1998: p. 2073-2076.

[5]   Zhang, M., Shi, L., Yuan, S., Zhao, Y. and Fang, J., Synthesis and photocatalytic properties of highly stable and neutral TiO_2/SiO_2, hydrosol. *J. Colloid Interf. Sci.,* 2009. 330: p. 113-118.

[6]   Periyat, P., Bajiu, K. V., Mukundan, P., Pillai, P. K. and Warrier, K. G. K., High temperature stable mesoporousanatase TiO_2photocatalyst achieved by silica addition. *Appl. Catal. A: General,* 2008. 349: p. 13-19.

[7]   Cao, A., Lu, R. and Veser G., Stabilizing metal nanoparticles for heterogeneous catalysis. *Phys. Chem. Chem. Phys.,* 2010. 12: p. 13499-13510.

[8]   Park, J., Aliaga, C., Renzas, J., Lee, H. and Somorjai, G., The role of organic capping layers of platinum nanoparticles in catalytic activity of CO oxidation. *Catal.Lett.,* 2009. 129: p. 1-6.

[9]   Arnal, P. M., Comotti M. and Schüth F., High-temperature-stable catalysts by hollow sphere encapsulation. *Angew.Chem.,* Int. Ed., 2006. 48: p. 8224-8227.

[10] Suryanarayanan, V., Nair, A. S., Renjis, T. T. and Pradeep, T., Porosity of core–shell nanoparticles. *J. Mater. Chem.,* 2004. 14: p. 2661-2666.

[11] Stark, W. J. and Pratsinis, S. E., Aerosol flame reactors for manufacture of nanoparticles. *Powder Technol.,* 2002. 126: p. 103-108.

[12] Fotou, S. E. and Pratsinis, S. E., Aerosol-made titania for photocatalytic destruction of organics, *J. Aerosol Sci.,* 1995. 26: p. 227-228.

[13] Pratsinis, S. E., Zhu, W. and Vemury S., The role of gas mixing in the flame synthesis of titania powders. *Powder Technol.,* 1996. 86: p. 87-93.

[14] Pratsinis, S. E., Flame aerosol synthesis of ceramic powders. *Prog. Energy Combust.Sci.,* 1997. 24: p. 197-219.

[15] Mädler, L., Kammler, H. K., Mueller, R., Pratsinis, S. E., Controlled synthesis of nanostructured particles by flame spray pyrolysis. *J.Aerosol Sci.,* 2002. 33: p. 369-389.

[16] Suh, J. S., Kim, C. S., Kim, T. O. and Choi M. S., Structural and chemical characterization of SiO_2/TiO_2 multicomponent particles during aerosol formation in a coflow diffusion flame. *Adv. Powder Technol.,* 2006. 17: p. 495-508.

[17] Lee, G. W. and Choi, S. M., Thermal stability of heat-treated flame-synthesized anatase TiO_2 nanoparticles. *J. Mater. Sci.,* 2008. 43: p. 715-720.

[18] Sheen, S., Yang, S., Jun, K. and Choi, M., One-step flame method for the synthesis of coated composite nanoparticles. *J. Nanopart. Res.,* 2009.

[19] Yang, S., Jang, Y.-H., Kim, C. H., Hwang, C., Lee, J., Chae, S., Jung, S. and Choi, M., A flame metal combustion method for production of nanoparticles. *Powder Technol.,* 2010. 197: p. 170-176.

[20] Hsu, C. W., Wang, L. and Su. W.F., Effect of chemical structure of interface modifier of TiO_2 on photovoltaic properties of poly(3-hexylthiophene)/TiO_2 layered solar cells. *J. Colloid Interf. Sci.,* 2009. 329: p. 182-187.

[21] Liu, Z., Zhang, X., Murakami, T. and Fujishima A., Sol–gel SiO_2/TiO_2 bilayer films with self-cleaning and antireflection properties. *Sol. Energ. Mat. Sol. C.,* 2008. 92: p. 1434-1438.

[22] Yuranova, T., Sarria V., Jardim, W.,Rengifo,J.,Pulgarin, C.,Trabesinger, G. and Kiwi, J., Photocatalytic discoloration of organic compounds on outdoor building cement panels modified by photoactive coatings. *J. Photoch. Photobio.A,* 2007. 188: p. 334-341.

[23] Akira Fujishima and Zhang, X., Titanium dioxide photocatalysis: present situation and future approaches. *C. R. Chimie,* 2006. 9: p. 750-760.

[24] Fujishima, A., Rao, T. N. and Tryk, D. A., Titanium dioxide photocatalysis. *J. Photoch. Photobio. C,* 2000. 1: p. 1-21.

[25] Fujishima, A., Zhang, X. and Tryk, D. A., Heterogeneous photocatalysis: Fromwater photolysis to applications in environmental cleanup. *Int. J. Hydrogen Energ.,* 2007. 32: p. 2664-2672.

[26] El-Toni, A. M., Yin, S. and Sato, T., Control of silica shell thickness and microporosity of titania–silica core–shell type nanoparticles to depress the photocatalytic activity of titania. *J. Colloid Interf. Sci.,* 2006. 300: p. 123-130.

[27] Teleki, A., Akhtar, M. K. and Pratsinis S.E., The quality of SiO_2-coatings on flame-made TiO_2-based nanoparticles. *J. Mater. Chem.,* 2008. 18: p. 3547-3555.

[28] Jian, S., Fouto, G. P. and Kodas T. T., A theoretical study on gas-phase coating of aerosol particles. *J. Colloid Interf. Sci.,* 1997. 185: p. 26-38.

[29] Gribb, A. A. and Banfield, J. F., Particle size effects on transformation kinetics and phase stability in nanocrystalline TiO_2. *Am. Mineral.,* 1997. 82: p. 717-728.

[30] Shannon, R. D. and Pask, J. A., Toptaxy in the anatase-rutile transformation. *Am. Mineral.,* 1964. 49: p. 1707-1717.

[31] Zhang, H., Chen, B. and Banfield J. F., The size dependence of the surface free energy of titania nanocrystals. *Phys. Chem. Chem. Phys.,* 2009. 11: p. 2553-2558.

[32] Balázs, N., Srankó, D.F., Dombi, A., Sipos, P. and Mogyorósi, K., The effect of particle shape on the activity of nanocystalline TiO_2photocatalysts in phenol deconposition. Part 2: The key synthesis parameters influencing the particle shape and activity. *Appl. Catal. B: Environ.,* 2010. 96: p. 569-576.

[33] Mogyorósi, K., Balázs, N.,Srankó, D.F., Tombácz, E., Dékány, I., Oszkó, A., Sipos, P. and Dombi, A., The effect of particle shape on the activity of nanocrystalline TiO_2photocatalysts in phenol decomposition. Part 3: The importance of surface quality. *Appl. Catal. BEnviron.,* 2010. 96: p. 577-585.

[34] Balázs, N., Mogyorósi, K., Srankó, D.F., Pallagi, A., Alapi, T., Oszkó, A., Dombi, A. and Sipos, P., The effect of particle shape on the activity of nanocrystalline TiO_2photocatalysts in phenol decomposition. *Appl. Catal. B: Environ.,* 2008. 84: p. 356-362.

[35] Jang, H. D., Kim, S.-K. and Kim, S.-J., Effect of particle size and phase composition of titanium dioxide nanoparticles on the photocatalytic properties. *J. Nanopart. Res.,* 2001. 3: p. 141-147.

[36] Zhang, J.-P., Shi, L.-Y., HU, Y.-Y. and Pan, Q.-Y., Morphology and photocatalytic activity of nanosizedtitania particles. *J. Shanghai Univ.,* 2001. 5: p. 247-252.

[37] Akurati, K. K., Vital, A., Fortunato, G., Hany, R., Nueesch, F. and Graule, T., Flame synthesis of TiO$_2$ nanoparticles with high photocatalytic activity. *Solid State Sci.,* 2007. 9: p. 247-257.

[38] Yeha, C.L., Yeh, S.H. and Ma, H.K., Flame synthesis of titania particles from titanium tetraisopropoxide in premixed flames. *Powder Technol.,* 2004. 145: p. 1-9.

[39] Katzer, M., Weber, A.P. and Kasper, G., The effects of electrical fields on growth of titaniaparticlesformed in a CH$_4$-O$_2$ diffusion flame. *J. Aerosol Sci.,* 2001. 32: p. 1045-1067.

[40] Vemury, S and Pratsinis, S.E., Charging and coagulation during flame synthesis of silica. *J. Aerosol Sci.,* 1996. 27: p. 951-966.

[41] Pratsinis, S. E., Artelt, C., Sanders, S. and Spicer, P.T., Flame aerosol synthesis of carbon and carbon-silica nanostructured particles.*J. Aerosol Sci.,* 1997. 28: p. 753-754.

[42] Zhang, H. and Banfield, J.F., Phase transformation of nanocrystalline anatase-to-rutile via combined interface and surface nucleation. *J. Mater. Res.,* 2000. 15: p. 437-448.

[43] Ramaswamy, V., Jagtap, N.B., Vijayanand, S., Bhange, D. S. and Awati, P.S., Photocatalytic decomposition of methylene blue on nanocrystalline titania prepared by different methods. *Mater. Res. Bull.,* 2007. 43: p. 1145-1152.

[44] Li, W., Bai, Y., Liu, C., Yang, Z., Feng, X., Lu, X., van der Laak, N. K. and Chan, K.-Y., Highly thermal stable and highly crystalline anatase TiO$_2$ for photocatalysis. *Environ. Sci. Technol.,* 2009. 43: p. 5423-5428.

[45] Jie, H.S., Park, H., Kim, K.H., Ahn, J.P. and Park, J. K., In-situ TEM observation on phase formation of TiO$_2$ nanoparticle synthesized by flame method. *Mater. Sci. Forum,* 2007. 534-536: p. 81-84.

[46] Zhang, H. and Banfield, J.F., Kinetics of crystallization and crystal growth of nanocrystallineanatase in nanometer-sized amorphous titania. *Chem. Mater.,* 2002. 14: p. 4145-4154.

[47] Nakaso, K., Okuyama, K., Shimada, M. and Pratsinis, S. E., Effect of reaction temperature on CVD-made TiO$_2$ primary particle diameter. *Chem. Eng. Sci.,* 2003. 58: p. 3327-3335.

[48] Zhang, H. and Banfield, J. F., New kinetic model for the nanocrystalline anatase-to-rutile transformation revealing rate dependence on number of particles. *Am. Mineral.,* 1999. 84: p. 528-535.

[49] Kobata, A., Kusakabe, K. and Morooka, S., Growth and Transformation of TiO$_2$ Crystallites in Aerosol Reactor. *AIChE Journal,* 1991. 37: p. 347-359.

[50] Lehtinen, K. E.J. and Zachariah, M.R., Energy accumulation in nanoparticle collision and coalescence processes. *J. Aerosol Sci.,* 2002. 33: p. 357-368.

[51] Zhang, H. and Banfield, J.F., Understanding polymorphic phase transformation behavior during growth of nanocrystalline aggregates: Insights from TiO$_2$. *J. Phys. Chem.* B, 2000. 104: p. 3481-3487.

[52] Mahdjoub, N., Allen, N., Kelly, P. and Vishnyakov, V., SEM and Raman study of thermally treated TiO$_2$anatasenanopowders: Influence of calcination on photocatalytic activity. *J. Photoch. Photobio.A,* 2010. 211: p. 59-64.

[53] Perego, C., Revel, R., Durupthy, O., Cassaignon, S. and Jolivet, J.-P., Thermal stability of TiO_2-anatase: Impact of nanoparticles morphology on kinetic phase transformation. *Solid State Sci.,* 2009.

[54] Choi, E. H., Hong, S.-I.and Moon, D. J., Preparation of thermally stable mesostructurednano-sized TiO_2 particles by modified sol–gel method using ionic liquid. *Catal Lett,* 2008. 123: p. 84-89.

[55] Hofer, M. and Penner, D., Thermally stable and photocatalytically active titania for ceramic surfaces. *J. Europ. Ceram.Soc.,* 2011. 31: p. 2887-2896.

[56] He, C., Tian, B. and Zhang, J., Thermally stable SiO_2-doped mesoporous anatase TiO_2 with large surface area and excellent photocatalytic activity. *J. Colloid Interf.Sci.,* 2010. 344: p. 382-389.

[57] Okada, K., Yamamoto, N., Kameshima, Y. and Yasumori, A., Effect of silica additive on the anatase-to-rutile phase transition. *J. Am. Ceram. Soc.,* 2001. 84: p. 1591-1596.

[58] Gellermann, C.,Ballweg, T.and Wolter, H., Herstellung von funktionalisierten oxidischen Nano- und Mikropartikeln und deren Verwendung. *Chem. Ing. Tech.,* 2007. 79: p. 233-240.

[59] Nádia, R.C., Fernandes, M. and Santana, V. S., Influence of thermal treatment on the structure and photocatalytic activity of TiO_2 P25. *Catal. Today,* 2005. 107-108: p. 5915-601.

[60] Furlong, D. N., Sing, K. S. W. and Parfitt, G. D., The precipitation of silica on titanium dioxide surfaces: I. Preparation of coated surfaces and examination by electrophoresis, *J. Colloid Interf. Sci.,* 1979. 69: p. 409-419.

[61] Binder, A. and Seipenbusch, M., Stabilization of supported Pd particles by the application of oxide coatings. *Appl. Catal. A: General,* 2011. 396: p. 1-7.

[62] Nishibori, M.,Shin, W., Tajima, K., Houlet, L.F., Izu, N., Itoh, T. and Matsubara, I., Long-term stability of Pt/alumina catalyst combustors for micro-gas sensor application. *J. Europ. Ceram. Soc.,* 2008. 28: p. 2183-2190.

[63] Hoffmann, M. R., Martin, S.T., Chiow. And Bahnemann, D. W., Environment applications of semiconductor photocatalysis. *Chem. Rev.,* 1995. 95: p. 69-96.

[64] Tobaldi, D. M., Tucci, A., Skapin, A. S. and Esposito, L., Effects of SiO_2 addition on TiO_2 crystal structure and photocatalytic activity. *J. Europ. Ceram. Soc.,* 2010. 30: p. 2481-2490.

[65] Colmenares, J. C., Luque R., Campelo, J. M., Colmenares, F., Karpiński, Z. and Romero, A. A., Nanostructured photocatalysts and their applications in the photocatalytic transformation of lignocellulosic biomass: An overview. *Mater. Lett.,* 2009. 2: p. 2228-2258.